ψ°	n	k	$10^3 \cdot \Delta(H^{-1})$, Oe^{-1}	m^*/m	ψ°	n	k	$10^3 \cdot \Delta(H^{-1})$, Oe^{-1}	m^*/m
0	12	12	0.47	0.60	67.5	6	6	0.95	0.30
	6	5	0.36	0.78		15	7	0.19	2.4
	5	4	0.52	0.54		8	5	0.31	0.91
	5	4	0.60	0.47		4	4	1.06	0.27
22.5	13	13	0.40	0.70	90	12	10	1.04	0.27
	2	2	0.34	0.83		12	7	0.32	0.88
45	24	23	0.23	1.2		8	5	1.10	0.26
	34	19	0.033	8.5					

ψ is the angle between the field vector and the tetragonal crystal axis, n is the highest order of resonance observed in a given series, k is the number of identified resonances of the given series.

of $X^{-1}\partial X/\partial H$, however they must coincide with the periods in the variation of X(H). The effective masses of the electrons have been computed by means of the following formula

$$m^*/m = (e/mc\omega)/\Delta(H^{-1}).$$

For each orientation ψ we have first tabulated the main series of deep resonances. The quantity m*/m is determined with an error of $\lesssim$ 2%, primarily as a result of the inaccuracy in the measurement of H. The error in the values of ψ amounts to $\sim 2^\circ$.

An analysis of the shapes and amplitudes of the resonance peaks is for the time being still premature due to a number of experimental reasons (inexact adjustment of the field, uneven surface of the single crystal etc.). However, certain regularities are apparent: for example in Fig. 1 the even resonances are deeper than the odd ones, which, possibly, may be explained by the effective mass being equal to exactly one-half. An investigation of these regularities will undoubtedly be useful in constructing the Fermi surfaces.

The author is grateful to P. L. Kapitza and A. I. Shal'nikov for unfailing interest in and attention to his work, and to G. S. Chernyshev for technical aid.

[1] M. Ya. Azbel' and É. A. Kaner, JETP **30**, 811 (1956); Soviet Phys. JETP **3**, 772 (1956). M. Ya. Azbel' and É. A. Kaner, JETP **32**, 896 (1957); Soviet Phys. JETP **5**, 730 (1957).

[2] E. Fawcett, Phys. Rev. **103**, 1582 (1956).

[3] P. A. Bezuglyĭ and A. A. Galkin, JETP **33**, 1076 (1957); Soviet Phys. JETP **6**, 831 (1958). P. A. Bezuglyĭ and A. A. Galkin, JETP **34**, 236 (1958); Soviet Phys. JETP **7**, 163 (1958).

[4] Kip, Langenberg, Rosenblum, and Wagoner, Phys. Rev. **108**, 494 (1957).

[5] V. B. Zernov and Yu. V. Sharvin, JETP **36**, 1038 (1959); Soviet Phys. JETP **9**, 737 (1959).

[6] M. S. Khaĭkin, Thesis, Inst. Phys. Prob. Acad. Sci. U.S.S.R., 1952.

Translated by G. Volkoff
295

MEASUREMENT OF ANGULAR DISTRIBUTIONS OF NEUTRONS ELASTICALLY SCATTERED FROM He^3

A. I. ABRAMOV

Submitted to JETP editor August 1, 1959

J. Exptl. Theoret. Phys. (U.S.S.R.) **37**, 1476-1478 (November, 1959)

To measure the angular distributions of neutrons elastically scattered from He^3 nuclei, we used a miniature spherical ionization chamber, filled with a mixture of 25% He^3 and 75% argon to a total pressure of 11 atmos.[1] As is well known, in elastic scattering the energy of the recoil nucleus ($E_{r.n}$) is linearly dependent on the cosine of the scattering angle of the neutron in the center-of-mass system

$$E_{r.n} = {}^1/_2 E_{max}(1 - \cos\theta),$$

where E_{max} is the maximum energy that can be transferred to the recoil nucleus. Therefore the energy distribution of the recoil nuclei is proportional to the differential scattering cross section in the c.m.s. and consequently the spectrum of the pulses due to the recoil nuclei yields directly the angular distribution curve for the argument $\cos\theta$. The angular distribution of elastic scattering of neutrons from He^4 was measured in an analogous manner. In the case of He^3 the measurements are made more difficult by the exothermal reaction $He^3(n, p)T^3$ (Q = 770 kev) which proceeds in paral-

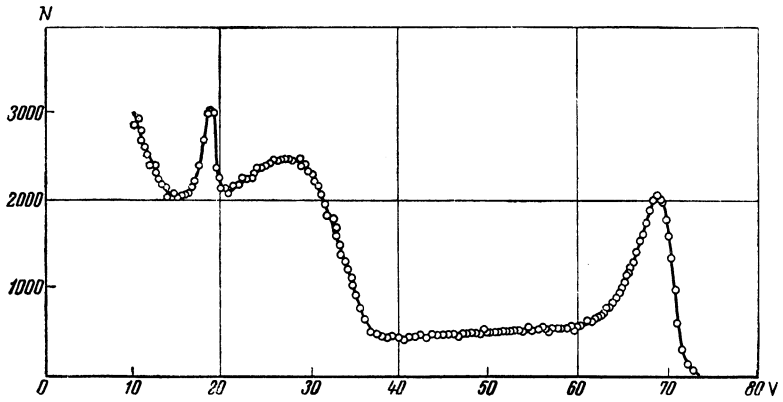

FIG. 1. Spectrum of pulses from an ionization chamber with He^3, bombarded by monochromatic 2 Mev neutrons. Abscissas – amplitude of amplifier output pulse (volts), ordinates – number of pulses per channel.

lel with the elastic scattering. The products of these reactions also produce pulses in the chamber, and complicate the picture of the pulse spectrum. Figure 1 shows a typical pulse spectrum from a chamber with He^3, taken at a proton energy of 2000 kev. On the right we see a peak from the reaction $He^3(n, p)T^3$, induced by the fast neutrons, on its left a "tail" due to the wall effect, and still farther on the left a hump due to the recoil nuclei with a superposed peak from the reaction $He^3(n, p)T^3$, induced by the slow neutrons that have passed through the cadmium. Thus, in the region of appearance of the recoil nuclei, the experimentally observed pulse spectrum must be separated into at least three components. In the present investigation the separation was made graphically, on the basis of spectra obtained with thermal neutrons. The form of the "tail" due to the fast peak was determined both by calculation and by plotting the thermal-neutron pulse spectrum at reduced working-mixture pressure, adjusted to make the range of the protons (and consequently also the magnitude of the wall effect) the same as in the case of the full working pressure and fast neutrons. After eliminating the pulses due to the (n, p) reaction with thermal and fast neutrons we obtained the pure spectra of pulses due to recoil nuclei, used to plot the angular distributions. A certain indeterminacy, which arises in subtraction of the spectra, is included in the experimental errors indicated on the graphs.

The measurements were made at neutron energies of 1000, 1400, 1800, 2000, 2770, and 4480 kev. The neutrons were obtained with an electrostatic Van de Graaff accelerator through the reactions $T^3(p, n)He^3$ (first four energies) and $D(d, n)He^3$ (last two energies). A standard linear amplifier

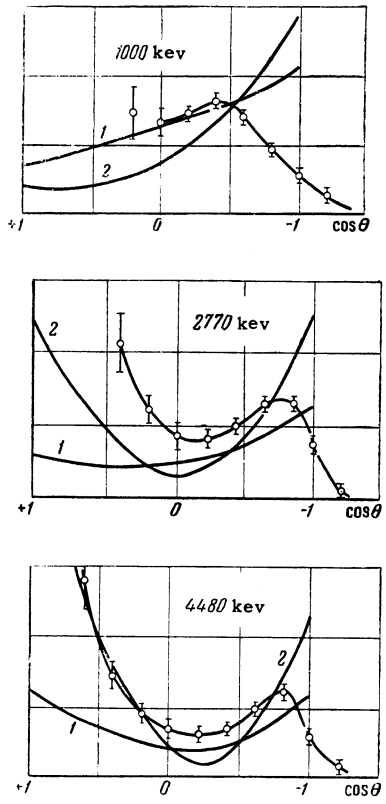

FIG. 2. Angular distributions of neutrons elastically scattered by He^3 nuclei.

and a 128-channel amplitude analyzer with ferrite memory were used.

The results of the measurement at neutron energies of 1000, 2770, and 4480 kev are given in Fig. 2, where the horizontal axis represents the cosine of the scattering angle in the center of mass system, and the vertical axis represents the differential scattering cross section in arbitrary units. The circles on the experimental curves show the readings of certain channels of the analyzer, with the total experimental error indicated. For comparison, the plots show the angular distributions calculated for the case of central forces, under two different assumptions concerning the character of the exchange interaction:[3] curve 1 for symmetrical interaction and curve 2 — for interaction of the Serber type (it must be noted that the curves given in Fig. 2 have been calculated for neutron energies of 1000, 2500, and 5000 kev respectively). In spite of the considerable discrepancy between the experimental and theoretical curves, it can be seen that a Serber-type interaction is in better agreement with experiment, at least at high energies. The data obtained in these investigations are used to interpret complex pulse spectra in spectrometric measurements with fast neutrons over wide energy ranges.

The author is grateful to O. D. Kazachkovskiĭ

and V. S. Stavinskiĭ for interest in the present work, and also to M. G. Yutkin, who participated in the preparation for the measurements.

[1] A. I. Abramov, Приборы и техника эксперимента (Instruments and Meas. Engg.) No. 4, 56 (1959).
[2] R. K. Adair, Phys. Rev. **86**, 155 (1952).
[3] Bransden, Robertson, and Swan, Proc. Phys. Soc. **A69**, 877 (1956).

Translated by J. G. Adashko
296

ON THE PIONIC AND ELECTROMAGNETIC STRUCTURE OF NUCLEONS

B. B. DOTSENKO

Physics Institute, Academy of Sciences, Ukrainian S.S.R.

Submitted to JETP editor August 7, 1959

J. Exptl. Theoret. Phys. (U.S.S.R.) **37**, 1478-1479 (November, 1959)

ACCORDING to the Blokhintsev-Jastrow[1] model, the nucleon consists of a dense core and a more porous pion cloud. The basic states characterizing the electromagnetic structure of the nucleons are considered to be two- and three-pion states, whose diagrams are given in Fig. 1 (references 2 and 3).

The two-pion state can be easily calculated, but a rigorous calculation of the three-pion state is very difficult.[2] Therefore, we use phenomenological considerations to describe this state. Considering that the external field has a relatively weak influence on the nucleon structure, we disregard the presence of the photon (dotted line in Fig. 1). Then, instead of a two-pion state we get a one-pion state, described by the plain Klein-Gordon[4] equation (with a delta-function source). On going to the three-pion state we suppose that an emitted virtual pion which has gone a distance of $\sim\hbar/\mu c$ from the core makes a transition during its lifetime of $\sim\hbar/\mu c^2$ to a new, "polarized" state which reveals its structural properties (a bound nucleon-antinucleon pair, or "loop")* and through these interacts with the core, according to the Chew hypothesis, on the basis of a single-pion exchange.[5] One of the simplest diagrams of such a process is given in Fig. 1b.

Neglecting the photon, and supposing that the beginning (emitted) and the final (absorbed)

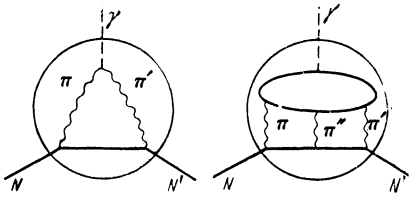

a b

FIG. 1. a – two-pion state; b – three-pion state. Solid straight line – nucleon N; wavy line – virtual pion π; dotted line – photon γ.

pions are the same, we can write down the equation for the wave function Ψ of such a Π pion interacting with the core through a single-pion exchange, that is, by the Yukawa rule:

$$\Delta\Psi + (\hbar c)^{-2}[(E - V(r))^2 - (mc^2)^2]\,\Psi = 0,$$
$$V(r) = -(g_\Pi g_c / r)\exp(-\mu c r/\hbar); \qquad (1)$$

the right side is zero, since nucleon regions far from the core are considered. The solution of this equation has the form[6,8]

$$\Psi = \exp[-i\varepsilon t/\hbar]\,Y(\vartheta,\varphi)\,R(r),$$
$$R(r) = \exp(-r/r_0)\,(r/r_0)^j\,w(r/r_0),$$
$$\varepsilon = \varepsilon(n); \quad j = -1/2 \pm \sqrt{(l+1/2)^2 - \beta^2}. \qquad (2)$$

Here n is the principal quantum number; l, the orbital quantum number; $\beta = g_c g_\Pi/\hbar c$; g_c is the nucleonic charge of the core; g_Π, the nucleonic charge of the Π pion; $Y(\theta, \varphi)$ is the angular part of Ψ; and the function $w(r/r_0)$ goes rapidly to a constant a_0.

From $j \geq 0$ (Ψ has no pole at zero) we get $l \geq 1$, i.e., the lowest state of such a system is a p state. If the density of the Π-pion cloud $D = \Psi^2$, $j = 0$ (reference 3) then $g_\Pi \sim 0.1\,g_c$. If we consider that the mass of the Π - pion m ~ M, then it is necessary, in considering the core — Π - pion model, to take the core motion into account.[7] In the "semiclassical" approximation we get (according to Sommerfeld[7]) expressions for the wave functions of the Π pion and the core, Ψ_Π and Ψ_c, in the center of mass system and the corresponding densities

$$D_\Pi = C_\Pi \exp(-r/a_\Pi), \quad D_c = C_c \exp(-r/a_c), \qquad (3)$$

where $a_\Pi \approx 0.23$ f, $a_c \approx 0.2$ f, and C_Π and C_c are constants (see reference 1).

The calculation of the mean square radius for the proton p and neutron n gives

$$\langle r\rangle_p^2 \approx \langle 0.76\,\phi\rangle^2, \quad \langle r\rangle_n^2 \approx \langle 0.19\,\phi\rangle^2$$
$$(1\,\phi = 10^{-13}\,\text{cm}). \qquad (4)$$

The results in (3) and (4) agree with references 1 and 3.